Available online at www.sciencedirect.com
SCIENCE DIRECT®
ELSEVIER
Ultramicroscopy 103 (2005) 165–172
ultramicroscopy
www.elsevier.com/locate/ultramic

On the measurement of lattice parameters in a collection of nanoparticles by transmission electron diffraction

C.T. Schamp, W.A. Jesser*

Department of Materials Science and Engineering, University of Virginia, 116 Engineer's Way, Charlottesville, VA 22904-4745, USA

Received 29 October 2003; received in revised form 28 October 2004; accepted 11 November 2004

Abstract

Improved accuracy in transmission electron diffraction measurements of interplanar spacings can be achieved by adding to the camera constant a term proportional to the square of the diffraction ring radius. A statistical technique using all of the diffraction rings yielded a precision better than 0.05% when measuring the lattice parameter of copper nanoparticles. Gold was used as an internal reference for copper by vapor depositing gold and copper on opposite sides of a thin amorphous carbon film. The source of the squared-radius term is consistent with distortions associated with the magnetic field of the post-objective lenses.

PACS: 07.78.+s

Keywords: Microscopic methods; Specifically for catalysts and small particles

1. Introduction

The measurement of lattice parameters of isolated nanoparticles suffers a strong disadvantage when using the normal method of X-ray diffraction as this technique inherently averages over a large region the size of the X-ray beam and produces low signal-to-noise ratios for very small particles. The transmission electron microscope (TEM) on the other hand is better suited in that it delivers a very narrow high-intensity beam to the sample for analysis. Malm and O'Keefe demonstrated through simulations that lattice imaging of nanoparticles by high-resolution electron microscopy is subject to errors as large as 10% because the measurement is highly sensitive to the tilt of the nanoparticle [1]. By imaging on a zone axis where two sets of lattice fringes are observed reduces the error in the measurement of the lattice parameter [2].

The technique of convergent beam electron diffraction (CBED) can be used to determine strains in crystals very accurately when HOLZ

*Corresponding author. Tel.: +1 434 982 5654; fax: +1 434 982 5660.
E-mail address: waj@virginia.edu (W.A. Jesser).

0304-3991/$ - see front matter © 2004 Elsevier B.V. All rights reserved.
doi:10.1016/j.ultramic.2004.11.007

lines in the central disk are considered, but this technique relies on crystals being between three and eight extinction distances thick [3]. For example, the extinction distance of the [1 1 1] beam from gold for a 100 keV electron is 18.3 nm [4], suggesting that nanoparticles should be at least 55 nm thick, which is beyond the size range of interest for many experiments.

If a region of nanoparticles with relatively uniform size and composition can be found, then the TEM technique of selected area electron diffraction (SAD) can be used to determine lattice parameters from a collection of particles. It is typically believed that measurements of lattice parameters by SAD is only about 2–3% accurate [5,6]. In cases where such accuracy is acceptable, it is sufficient to assume the diffraction ring radius R is inversely proportional to the interplanar spacing d_{hkl}. However, if greater accuracy is required, this assumption of linearity can be improved upon. Andrews et al. [7] suggest that by expanding the $\sin(\theta)$ term in Bragg's law to order R^2, a more accurate relationship between R and d_{hkl} can be derived. Lodder and van der Berg found the correction of Andrews et al. to be 10–20 times smaller than is experimentally found and suggest a stronger empirical correction factor [8]. Lodder and van der Berg use their approach to measure the lattice parameters of several metals by the SAD technique, and suggest that the accuracy of those measurements can be 0.1%.

The SAD technique is particularly good if one is to consider many different diffraction rings in a polycrystalline pattern. The main intention of the present paper is to present an improvement to the approach by Lodder and van der Berg, and to show how this technique can be applied to more precisely measure the lattice parameter(s) of a collection of nanoparticles. With the increased precision of measuring lattice parameters, a technique to measure anisotropic strain in a collection of nanoparticles is suggested.

2. Experimental details

99.9999% pure gold purchased from Alfa Aesar and 99.9995% pure copper purchased from Aldrich were thermally evaporated from tungsten wire baskets in a diffusion pumped vacuum chamber at ambient pressures of about 10^{-5} Torr. Gold and copper deposits grew as 10–100 nm islands on heated amorphous carbon films supported by 3 mm copper transmission electron microscope (TEM) grids. Gold standard diffraction calibration grids were purchased as well. The TED experiments were performed using a JEOL 2000FX TEM with the beam fully expanded in all experiments. Non-zero convergence experiments, as measured from the optic axis, were not considered.

2.1. Measurement considerations

To measure lattice parameters of a collection of nanoparticles by TED, one should have a known reference material to calibrate the measurements. Often, if accuracy is not very important, the camera length of an image is simply read from the display of the microscope. This technique is likely good to about 5% for a microscope that is maintained. One can calibrate the camera length by using a diffraction standard such as commercially available gold on holey carbon, and then exchange it for the sample of interest and try to align the microscope exactly as it was for the standard. For a skilled TEM user, this technique can obtain an accuracy of about 2% [5,6]. The most accurate calibration would have the sample and the standard in the microscope at the same time, with little or no translation required to obtain diffraction patterns from both materials, which effectively removes the requirement of a high degree of operator skill. To determine the best technique to measure lattice parameters of nanoparticles with an internal reference, three configurations of sample and reference are compared. These configurations are two semi-circular grids, two stacked grids and one grid using top and bottom film surfaces.

2.1.1. Two semi-circular grids

One possible configuration of a sample and a standard is to have two semi-circular grids, one as sample, the other as standard clamped side-by-side in a TEM sample holder. A diffraction pattern

from the standard would be recorded, then the holder would be translated in two or three dimensions so that diffraction patterns of the sample would be recorded. This technique prevents cross contamination of the sample and standard, but likely introduces errors associated with translation of the sample holder and refocusing the image of the sample with only the vertical height adjustment. This technique is similar to the technique of inserting a standard to calibrate the microscope parameters, and then inserting a sample and accurately relocate the same vertical position used for the calibration. Lodder and van der Berg had success with this approach [8], but its sensitivity depends on the skill of the operator.

The limiting factor in this technique is reproducibility of the sample position within the objective lens of the TEM. To determine the degree of the error associated with translating the sample holder, a diffraction calibration standard of gold on holey-amorphous carbon purchased from Ted Pella Inc. was used to obtain diffraction patterns from five widely spaced areas of the standard. The grid was tilted 15° from the horizontal to ensure that some vertical translation would be required after each of the lateral translations.

The reproducibility in this technique also depends on the skill of the operator as can be seen from the following data collected by this approach in Fig. 1. The error bars represent the error in λL of each diffraction pattern. In this case, four of the five positions have very nearly the same measurement in the camera constant, suggesting that this technique is about 80% reproducible. A more reproducible technique is desired to reliably measure lattice parameters through TED.

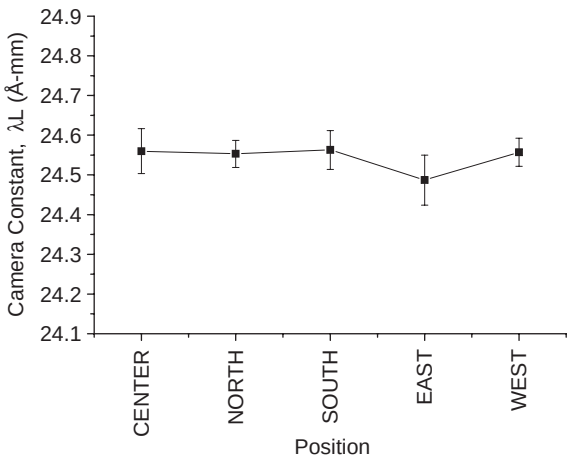

Fig. 1. Camera constant measured at various positions on a tilted TEM grid showing that the reproducibility of using a calibrated camera constant is strongly dependent on the skill of the operator.

2.1.2. Two stacked grids

A second possible configuration of standard and sample investigated was to stack two separate grids on top of one another. This has the advantage that the sample and reference materials can be separated by up to two grid thicknesses, thus minimizing the possibility of cross contamination. Two commercially available standards, one gold on holey-amorphous carbon, and another of thallous chloride were stacked in three different arrangements; materials facing opposite directions, materials facing the same direction, and the materials facing each other. It was found that none of these arrangements permitted both sets of diffraction patterns to be in focus simultaneously. In principle, the second diffraction pattern could be brought into focus with only the height adjustment, but this relies on the skill of the operator, which from Fig. 1 shows in this case an accuracy of about 80%. Therefore, this technique should not be considered as a good configuration for precise lattice parameter measurements.

2.1.3. One grid

The third configuration of the sample and standard investigated was that of a thick standard deposited on one side of an amorphous carbon film, and an unknown on the other side of the film. This is the method that gave the best results in terms of having both sets of diffraction patterns in focus. In this case, gold and copper were used as the standard and sample materials. By using a thick standard, the effects of surface stress on the lattice parameter of the standard can be neglected. An anneal at the deposition temperature of 500 °C for an hour in vacuum is performed to release residual stresses, but was found to retain a small residual strain along the [1 1 1] direction, as described later in the paper. This residual strain

seems to affect the scatter in the data more strongly than the averaged measurements, so the averaged lattice parameter measurements of gold are used as the standard.

This technique has the advantage of being able to simultaneously have both sets of diffraction patterns in focus, and is not very likely to yield cross contamination of the sample and the standard material. To determine the precision of this technique, the standard (gold) from the first side was used as a reference to determine the lattice parameter of the sample (copper) from the second side. This technique was found to be the best for accurate determination of lattice parameters and will be the subject of the remainder of the paper. First, the approaches to locating diffraction peak positions and measuring the ring radii are presented.

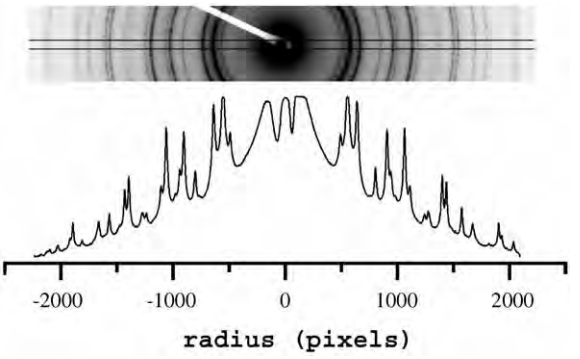

Fig. 2. TED patterns from Au and Cu on opposite sides of an amorphous carbon film. The bar through the center indicates the 75 pixel tall intensity trace shown. The peaks in the intensity trace are fit to Lorentzian functions giving the peak center location and the standard deviation of the fit.

3. Analysis details and results

Using the one-grid technique or the gold standard alone, SAD patterns from islands of gold were recorded on negatives from a JEOL 2000FX TEM and scanned at 1200 dpi on a Umax PowerLook III scanner to obtain a digital pattern for processing. A 75 pixel tall scan across the SAD pattern was used to extract an intensity trace across the diffraction pattern (Fig. 2). Each point in the intensity trace is the average grayscale value of the 75 pixel height of the scan line. Using a 75 pixel height scan results in a smooth intensity trace, but shifts the peak center inward, proportional to the height of the intensity trace. The error associated with this inward shift for 75 pixels was calculated and found to be insignificant. The grayscale pixel values so generated were exported to the plotting program, Origin, where the peaks were fitted by Lorentzian curves to determine the center peak position. These peaks were correlated to corresponding *hkl* planes, and ring diameters were determined from the distances between corresponding peaks. It is instructive to note that by considering higher powers of the measured diffraction radius to determine d_{hkl}-spacings, the reciprocal length per scanned pixel is not constant, but smaller at larger measured radii. The range of particle size that is applicable for use by this technique is limited by diffraction line broadening for very small-size particles, and by too few diffraction spots contributing to the SAD rings due to a lower frequency of particles for large-size particles. In the present case a 75 pixel average produced sufficiently smooth peaks (Fig. 2).

The classical equation for SAD analysis relates the measured ring radius to the corresponding interplanar spacing, d_{hkl}, where the slope of a plot of d_{hkl} against R^{-1} gives the camera constant, λL. To obtain a better fit for the data, an iterative approach was used. While the data appear to lie very well on a straight line with nearly no scatter as is shown in Fig. 3, it can be demonstrated that the scale of the ordinate is too coarse to properly reveal the scatter in the data, or to show the error bars associated with each data point, which are smaller than the symbols on the plot.

The iteration starts by finding the slope λL from the linear least-squares fit to d_{hkl} vs. R^{-1} using zero for the d_{hkl} intercept where the d_{hkl} values used are the bulk values. Then a revised set of d_{hkl} values is found for each ring based on

$$d_{hkl} = \frac{\lambda L}{R}, \tag{1}$$

where the λL from the above least-squares fit is used. The average lattice parameter, $\bar{a}$, is determined from the m measured R values using the

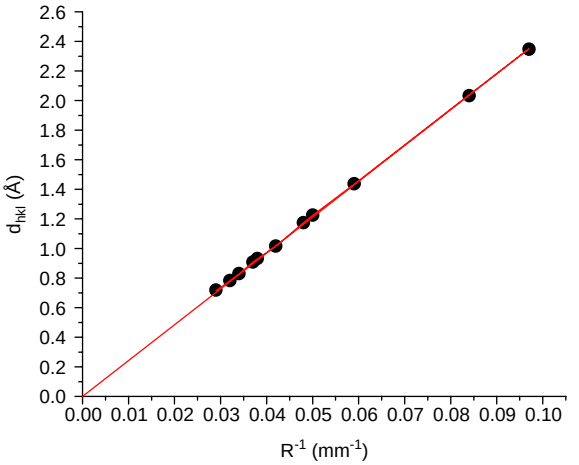

Fig. 3. Measured interplanar d-spacing for each ring plotted against inverse ring radius. The scale of this plot is too coarse to show the scatter in the data.

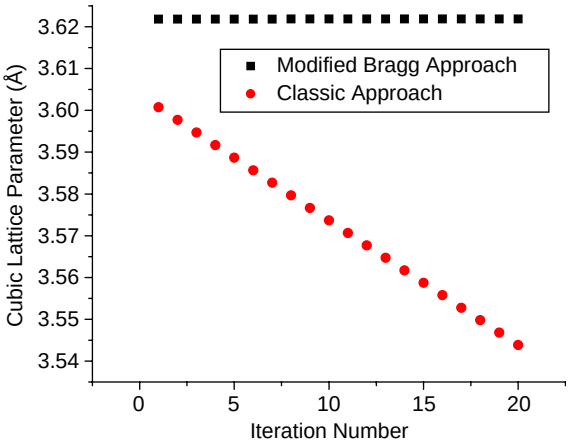

Fig. 4. Lattice parameter of gold calculated by the classic and modified Bragg approaches plotted against the number of iterations used to calculate the lattice parameter. The classic approach calculates a smaller lattice parameter with each iteration, indicating that the classic model does not improve with the number of iterations.

equation for cubic structures:

$$\bar{a} = \frac{1}{m}\sum_{i=1}^{m}\frac{\lambda L}{R_i}\sqrt{(h^2+l^2+k^2)}. \tag{2}$$

Using the $\bar{a}$ from Eq. (2) instead of the bulk value, the procedure is repeated to find a second λL value from which a second $\bar{a}$ is obtained.

Interestingly, the average lattice parameter is found not to converge to a best fitting value, but decreases linearly with the iteration as is shown in Fig. 4. Andrews et al. [7] suggested that a better approach is to expand the $\sin(\theta)$ term in Bragg's law, and drop higher-order terms, which to first order the relationship between d and R is

$$Rd = \lambda L + \left(\frac{3}{8}\frac{\lambda}{L}\right)R^2. \tag{3}$$

Lodder and van der Berg [8] pointed out that the coefficient, $\frac{3}{8}\lambda/L$, to the R^2 term is about an order of magnitude smaller than that found experimentally at typical SAD camera lengths and suggested using the empirical equation

$$Rd = \lambda L + kR^2 \tag{4}$$

which worked well. From this point on in the paper, use of this equation will be referred to as the modified Bragg approach and the use of this

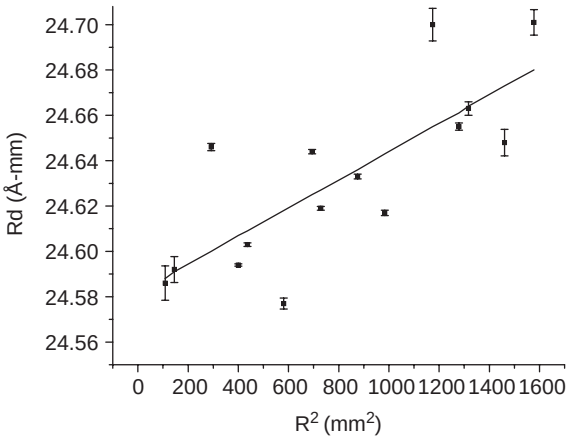

Fig. 5. Modified Bragg approach applied to the same gold diffraction pattern as Fig. 3. From this plot, the apparent scatter in the data becomes evident by the finer scale used here.

equation with $k = 0$ will be referred to as the classical approach.

To determine k and λL for the modified Bragg approach, Rd is plotted against R^2, yielding a plot of slope k and intercept λL (Fig. 5). The error bars in Fig. 5 represent the standard deviation of the fit to the corresponding peak in the SAD pattern. Just as in the case for the classical approach, k and

λL are found by an iterative least-squares fit, so in the case of the modified Bragg approach, k and λL are determined by an iterative least-squares fit except now the average lattice parameter $\bar{a}'$ is given by the equation

$$\bar{a}' = \frac{1}{m}\sum_{i=1}^{m}\left[\left(\frac{\lambda L}{R_i} + kR_i\right)\sqrt{(h^2+k^2+l^2)}\right]. \quad (5)$$

As with the classical iterative approach, this average lattice parameter is used to determine a new set of d_{hkl}'s from Eq. (5) and then to obtain a new intercept λL and slope k. It was usually found that only two iterations gave a final value of $\bar{a}'$, and that further iterations altered the value in the part per million range.

After this iterative approach was used for the standard material to find the line of best fit by a least-squares analysis, and from that the best slope k, and the intercept λL for that data set, this k and λL are then used to determine the set of Rd's of the unknown material. A similar iteration is made to determine the best fitting lattice parameter of the unknown material. The best fitting set of d-spacings have now been determined separately for the standard and the unknown. For additional precision, both sets of data are plotted together on an Rd vs. R^2 plot where the slope k and intercept λL of the combined data set can be found. Finally, using the k and λL of the total data set, the lattice parameter of the unknown is determined once again. The advantage of this is that better statistical precision of the data can be achieved. This technique is used to determine the lattice parameter of copper from a gold standard (see Fig. 6), showing that the precision of the technique is 0.049%, where the precision is defined as the standard deviation of the entire data set normalized to the bulk lattice parameter. The copper lattice parameter measured by this technique is 3.621 Å as compared to 3.615 Å for bulk.

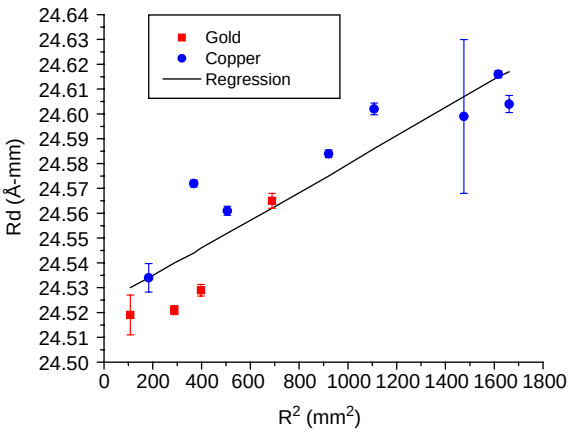

Fig. 6. Modified Bragg approach used with gold as an internal reference to measure the lattice parameter of copper. The precision in the measurement of the lattice parameter of copper using this technique is found to be better than 0.05%.

4. Discussion

4.1. Shift of center location

An interesting aspect of the measurements of the TED rings is that the center position of the TED pattern systematically shifts with increasing ring radii. This shift is calculated as the center position between the left and right ((hkl) and $(\overline{hkl})$) measured peak locations on the intensity trace. The effect is nearly negligible, at about 4 pixels or about 0.08 mm for a 1200 pixel/in scan. This effect is consistent with coma aberration of the objective lens [10].

4.2. Scatter in the data

When comparing the same data plotted with the classic and modified Bragg approached in Figs. 3 and 5 respectively, the modified Bragg approach deceptively appears to have a much greater degree of scatter in the data. This is due to the coarse scale of the ordinate used in the classical approach for d, as compared to the greatly expanded scale used in the modified approach thereby revealing scatter in the data.

In Fig. 4, the lattice parameter obtained by the modified Bragg approach is plotted against the number of iterations. Note that there is little change. However when the lattice parameter from the classical approach is plotted on the same figure with that obtained by the modified approach, the divergence in the classical approach is seen.

4.3. Nature of k

The expansion of Bragg's law to second order in R is given in Eq. (3) which does not include any effects associated with distortions or astigmatisms from the magnetic fields of the microscope lenses. Eq. (4) is an empirical equation which does permit the incorporation of the effects caused by distortions but its nature was not explained in the original literature [8,9].

To investigate the nature of k, a series of polycrystalline Au SAD patterns were recorded at different camera lengths. For each SAD pattern, k and L from Eq. (4) were determined using the procedure outlined above and plotted as k vs. L^{-1} in Fig. 7. In addition to this data, the coefficient of R^2 in Eq. (3), $(\frac{3}{8}\lambda)1/L$, is shown as a reference line. One can see that k has a negative non-linear slope, whereas the reference line has a positive linear slope. The difference between k and the reference line is due to the distortion from the intermediate and projector lenses in the TEM. It has been shown that aberrations result primarily from the objective lens, whereas distortions occur from the post-objective lens system [10], therefore k strongly depends on the currents of the intermediate and projectors lenses.

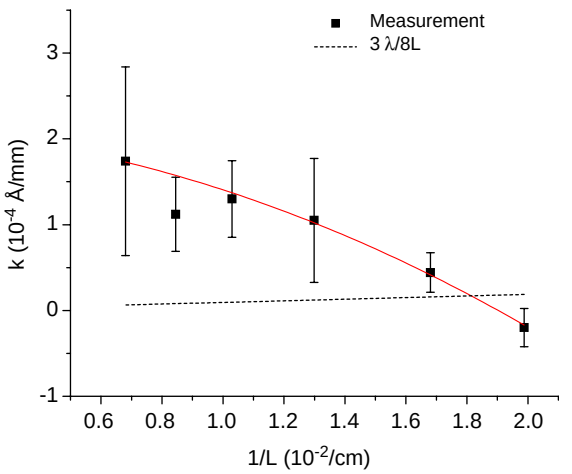

Fig. 7. R^2 coefficient, k, plotted against inverse camera length L^{-1} and the theoretical coefficient of R^2 as a reference line. From this plot, it is apparent that a camera length could potentially be chosen to give a value of zero for k, resulting in the classic equation being highly accurate, or k can be chosen at the intersection of the two lines, which would ensure agreement with the modified Bragg approach (Eq. (3)).

There are several sources of distortions as discussed in the books by Reimer and Hawkes that contribute higher-order terms in R to Eq. (3) [4,10]. No attempt has been made to quantify these, but rather to show that the coefficient of R^2 can be changed through the intermediate lens current, and hence L.

4.4. Extension to non-cubic lattices

This analysis is applicable to non-cubic crystal structures, as the model in its simplest description is a more accurate relationship between the measured SAD ring radii and the corresponding d_{hkl} spacings. A known standard material is required as an internal reference for this technique. Its rings should be measured and indexed, which after following the procedure outlined in this paper will give values for the initial k and λL, except that instead of using Eq. (5), it should be rederived for the appropriate crystal structure.

After determining the initial k and λL values, d_{hkl} values for the sample rings can be determined. After indexing these d_{hkl} values, a multi-variable least-squares regression can be used to find the best fitting lattice parameters.

4.5. Anisotropic strain in cubic gold

Most of the apparent random scatter in the lattice parameter derived from each ring can be accounted for by an elastic distortion of the cubic unit cell. The model for this elastic distortion is an expansion of the cubic unit cell along the [1 1 1] axis and a Poisson contraction in the plane normal to the [1 1 1] axis. The lattice parameter for each ring of the diffraction pattern is derived from an elastic distortion of $\varepsilon = 0.3\%$ along the [1 1 1] axis and the associated Poisson contraction of $-\upsilon\varepsilon$, where υ is 0.42 for bulk gold. The data from Figs. 3 and 5 are replotted as the lattice parameter against R^2, along with the best fitting value of $\varepsilon = 0.3\%$ for the model, and two other values of ε for comparison. These plots are shown in Fig. 8. For many of the data points, the general trend in the data is matched with the trend in the model. The

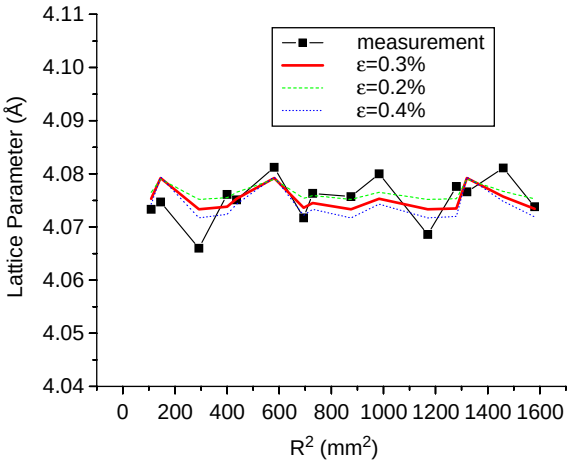

Fig. 8. Lattice parameter measured from each diffraction ring of gold plotted against R^2. The gold was modeled as having a 0.3% strain along the [1 1 1] direction, with the appropriate Poisson contraction resulting in a lattice parameter predicted for each ring that approximates the variations in the measured lattice parameter. Modeled lines of lesser quality fit for $\varepsilon =$ 0.2% and 0.4% are shown for comparison.

reason for the anisotropic strain in the gold particles after an anneal is likely to be a result of the disc morphology, i.e., high aspect ratios.

5. Conclusions

- By using higher-order terms with the classic Bragg law approach relating interplanar spacings to measured distances on a diffraction pattern and an internal reference, the lattice parameter of copper was measured with a precision of 0.05%.
- The origin of a correction term to the classic Bragg law in TED pattern can be attributed to deviations in the radial dependence of the magnetic field in the microscope lenses.

Acknowledgment

This work was supported primarily through the MRSEC Center for Nanoscopic Materials Design by the National Science Foundation under Award Number DMR-0080016.

References

[1] J.-O. Malm, M.A. O'Keefe, Ultramicroscopy 68 (1) (1997) 13–23.
[2] O'Keefe, private communication.
[3] B. Fultz, J.M. Howe, Transmission Electron Microscopy and Diffractometry of Materials, Springer, Berlin, 2002.
[4] L. Reimer, Transmission Electron Microscopy: Physics of Image Formation and Microanalysis, Springer, Berlin, 1997.
[5] D.B. Williams, C.B. Carter, Transmission Electron Microscopy: a Textbook for Materials Science, Plenum Press, New York, 1996.
[6] T.B. Rymer, Electron Diffraction, Butler & Tanner Ltd., Frome, 1970.
[7] K.W. Andrews, D.J. Dyson, et al., Interpretation of Electron Diffraction Patterns, Adam Hilger Ltd., Glasgow, 1971.
[8] J.C. Lodder, K.G. van der Berg, J. Microsc. 100 (1) (1974) 93–98.
[9] J.W. Edington, Practical Electron Microscopy in Materials Science, TechBooks, Herndon, 1976.
[10] P.W. Hawkes, E. Kasper, Principles of Electron Optics, Academic Press Limited, London, 1989.